Chapter 7
Turbidity at the Source: Aiming for Minimized Sediment Dispersion During Deep-Sea Mining

Rudy Helmons, Said Alhaddad, Claire Chassagne, Mohamed Elerian, Geert Keetels, Alex Kirichek, and Laurenz Thomsen

Abstract The chapter gives an overview of the sediment dispersion generated by the mining process. Within the field of dredging engineering, ample experience is available regarding equipment, turbidity generated by equipment, and sediment transport processes. High up the environmental impact mitigation hierarchy are avoidance and minimization. That is where engineering can provide (part of) the solution. It is our aim to predict and consider how we can improve the mining process and equipment. Within this context, our focus is on those processes that are likely to take place close to the seabed. On the one hand, our work focuses on the prediction and reduction of the amount of sediment that might get suspended. On the other hand, considering the conditions under which the suspended sediment might be released in the most optimal way to reduce dispersion, we have performed and analysed small-scale and full-scale laboratory experiments of a hydraulic collector design and various dynamic sedimentation experiments.

Keywords Particle aggregation · Polymetalic nodules · Sediment plume · Sediment pickup & deposition · Settling velocity

R. Helmons (✉)
Maritime and Transport Technology, Faculty of Mechanical, Maritime and Materials Engineering, Delft University of Technology, Delft, the Netherlands

Mineral Processing and HSE, Norwegian University of Science and Technology, Trondheim, Norway
e-mail: r.l.j.helmons@tudelft.nl

S. Alhaddad · M. Elerian · G. Keetels
Maritime and Transport Technology, Faculty of Mechanical, Maritime and Materials Engineering, Delft University of Technology, Delft, the Netherlands

C. Chassagne · A. Kirichek
Environmental Fluid Mechanics, Faculty of Civil Engineering and Geoscience, Delft University of Technology, Delft, the Netherlands

L. Thomsen
University of Gotheborg, Gothenburg, Sweden

R. Sharma (ed.), *Deep-Sea Mining and the Water Column*,
https://doi.org/10.1007/978-3-031-59060-3_7

1 Introduction

Polymetallic nodules have attracted interest from industry and scientists for several decades. As of the 1970s and 1980s of the last century, significant attempts have been made to collect nodules in an economic way. Nodules have attracted renewed interest over the last decade. Nowadays, the concern about the potential environmental impact of seabed mining has gained more attention. Industry will be challenged to work according to the best available technology and best environmental practices to minimize and mitigate the environmental impacts. It is not yet clear which technologies and methodologies will lead to the least environmental impact while still considering an economically viable mining operation.

Various solutions and technologies for exploitation are being developed. In general, any deep-sea mining system will consist of similar subsystems, i.e.:

1. Seafloor Mining Tool (SMT): Nodules need to be picked from the seabed.
2. Vertical Transport System (VTS): Nodules need to be transported to surface and excess water, sediment, and other effluents need to be transported subsea.
3. Mining Support Vessel (MSV): Nodules need to be separated from non-valuable materials. The nodules will be stored in the hold, while the non-valuable materials should be provided to the VTS to return back subsea.

In general, the material flow from the seabed to the mining vessel can be divided into four stages (Lang et al., 2019), see Fig. 7.1:

1. Seabed to seafloor mining tool
2. Seafloor mining tool to environment
3. Seafloor mining tool to mining vessel via a vertical transport system
4. Mining vessel to environment (seabed and/or water column) via a vertical transport system

Several processes occur simultaneously, influencing material flows 1 and 2. For most seafloor mining tools, it is expected that they will generate turbidity due to the machine manoeuvring on top of the seabed, e.g., sediments are suspended by the motion of the vehicle tracks. At the same time, as the SMT collects nodules, it will entrain water and sediment. Part of the entrained water and sediment will move through the collector and part of it will spill directly to the environment. Within the SMT, nodules will be separated from the excess water and sediment. The excess materials will then be expelled behind the collector vehicle, often referred to as collector or diffuser plume, see Fig. 7.2.

Various technology concepts exist, varying in their levels of maturity (Lesage, 2020). One of the tested technologies is that of The Metals Company and Allseas, as they successfully conducted an integrated field test in October 2022. Their system consists of a hydraulic (Coanda-effect-based) nodule collector, a riser-based airlift system, and the excess water and sediments on board of the MSV are discharged into the midwater column Nauru Ocean Resources Inc (2021). Similar concepts are developed by others, e.g. GSR (Ouillon et al., 2021), Royal IHC (Haalboom

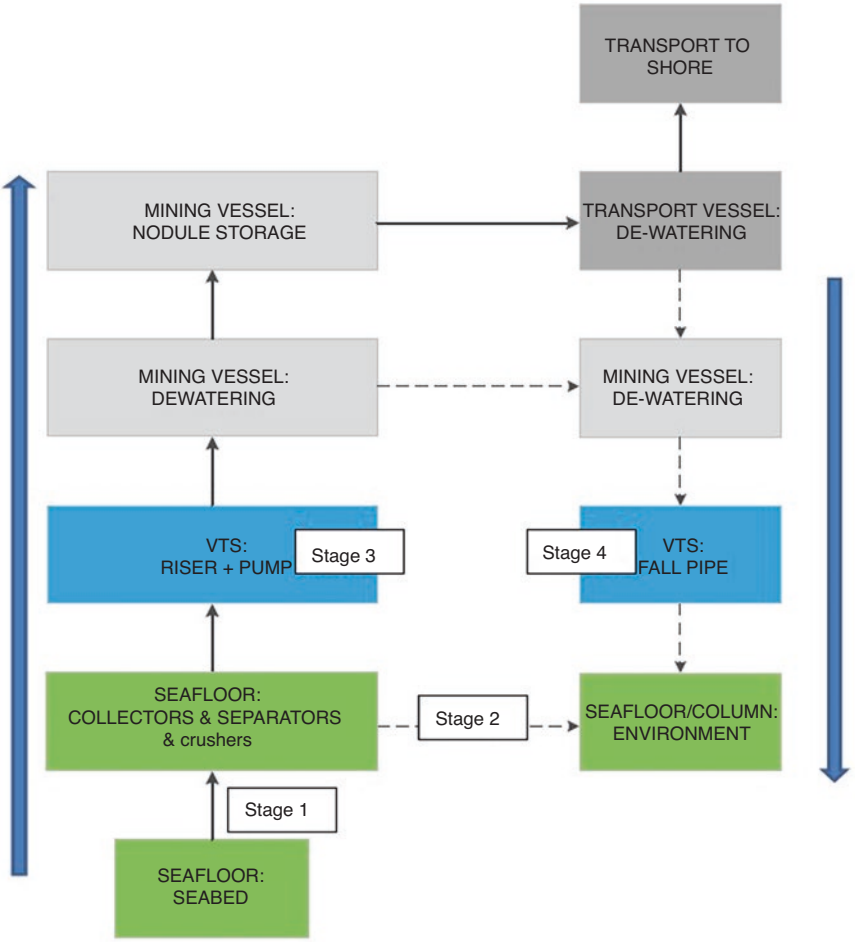

Fig. 7.1 Schematic of material flows. Solid lines represent the main flow (nodules) and dashed lines represent secondary flow (sediments, waste, and other effluants, SWOE). Blue arrows show the general direction of the flow. (Based on Blue Nodules Lang et al., 2019)

et al., 2023), based on other hydraulic concepts, e.g. KIOST (Hong et al., 2019), COMRA (Kang & Liu, 2021), or mechanical collection, e.g. NIOT (Atmanand and Ramadass, 2017). All such concepts can be grouped as continuous SMTs; that is, they are designed to effectively collect all nodules in the tool's pathway. There are other concepts under development that consider picking up individual nodules (Gillham, 2022), but such concepts are not yet demonstrated at a sufficiently high technology readiness level to be considered as available technology at the required economy of scale. Regarding VTS, most concepts are based on continuous transport systems, e.g., hydraulic (van Wijk, 2016) or airlift (NORI-D EIA, 2021), or discontinuous systems based on skip lifting of containers (van den Bosch, 2023).

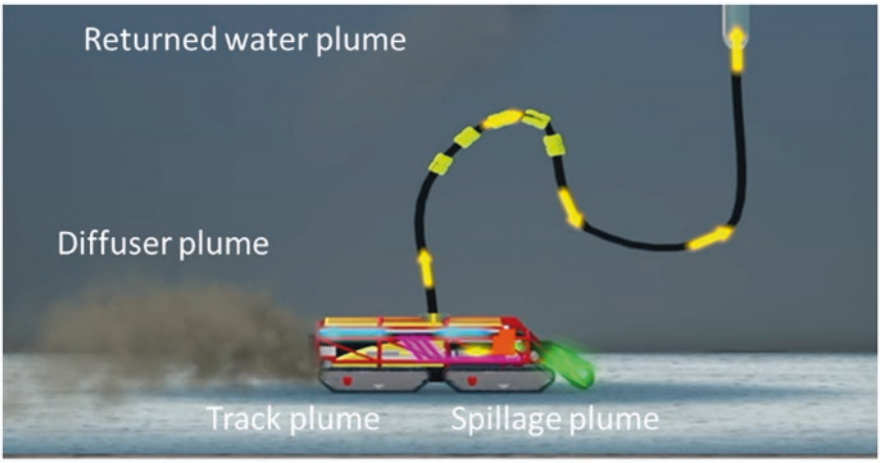

Fig. 7.2 Main source terms of turbidity generated near the bed. (Based on Blue Nodules Lang et al., 2019)

The continuous and discontinuous systems differ significantly in terms of the amount of water and potentially sediments that will be mobilized, transported to the surface, or separated to be released into the environment. For example, in hydraulic transport it is expected that approximately 12 % of the transported mixture consists of ore (van Wijk, 2016). This means that a large volume of water and sediment needs to be discharged subsea. So far, there is no consensus on whether the return flow needs to be discharged close to the seabed or whether it would be acceptable to be discharged midwater column. Some hydraulic transport concepts inherently require the return water flow to provide flow for drill-string-based systems, inherently discharging the excess water near the seabed (van den Bosch, 2023).

In this chapter, the emphasis will be on specific systems and/or physical phenomena relevant for the material flows identified in categories 1, 2, and 4 above. The experimental results that we will present are based on a variation of non-cohesive fine sediments and substitute cohesive sediments to unravel physical phenomena, allow for sufficient repetitions, and allow us to work with the limited availability of sediments collected from CCZ area. Several experiments have been executed with original CCZ sediment as well. In Sect. 2, a Coandă-effect-based nodule collection system is analysed for the physical phenomena occurring underneath the collector head. We will shed light on the pressure distribution and provide insights into the mechanisms that influence erosion of the bed. Various lab-scale tests have been conducted to investigate the near-bed release of the SWOE; these are discussed in Sect. 3. The next section discusses a combination of both simulations and experiments to further investigate the release conditions of a collector plume, in which the emphasis is on studying the effect that particle aggregation might have on the dispersion of the sediment plume, based on hydrodynamic flows such as lock-exchange as well as closed volume experiments in a sea-water column simulator.

2 Coandă-Effect-Based Nodule Collection System

Various hydraulic collection techniques were explored in the literature, including the suck-up-based approach (Zhao et al., 2019), double-jet method (Hong et al., 1999), and Coandă-effect-based method (Alhaddad et al., 2023). It is anticipated that the Coandă-effect-based collectors will cause less disturbance to sediments, as the flow from the nozzle of the collector does not directly interact with the seabed (Zhao et al., 2021). Consequently, this technology is being widely considered in the field of polymetallic-nodule mining. This section, therefore, provides an overview of the underlying physics of the collection mechanism using a Coandă-effect-based collector. Furthermore, directions towards minimizing the sediment collection by the collector are presented.

The Coandă effect, named after the Romanian scientist Henri Coandă, can be described as the tendency of a jet flow to remain attached to a nearby surface, even when this surface curves (Reba, 1966). A diagram illustrating the basic design of a Coandă-effect-based collector is depicted in Fig. 7.3. The design comprises a couple of ducts, a jet duct and a collection duct, which are formed by three curved surfaces. Due to the Coandă effect, the fast-moving water jet follows the contour of the upper curved plate. Consequently, surrounding water is entrained towards the collection duct, creating a pressure difference (suction) under the collector, kicking up nodules from the seabed and dragging them towards the collection duct. It should be noted that not only does the water jet entrain ambient water into the collection duct, but it also injects water behind the collector head, which is referred to as 'spilling water' (see Fig. 7.3).

In fact, polymetallic nodules are partially or completely embedded in the sediment of the ocean floor, meaning that sediments will unavoidably be dislodged and picked up along with the nodules during mining. Consequently, the sediments are discarded behind the hydraulic collectors, forming a sediment plume that can travel long distances and potentially disrupt aquatic ecosystems. In order to evaluate the

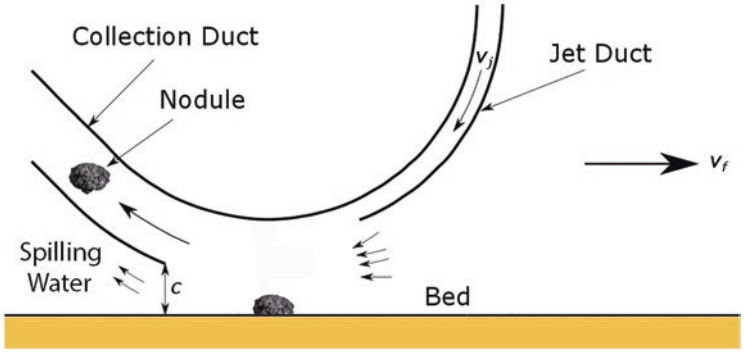

Fig. 7.3 Diagrammatic illustration of the collector head, where v_j represents the jet velocity, v_f represents the forward velocity of the collector, and c represents the clearance. The smaller arrows indicate the direction of water entrainment

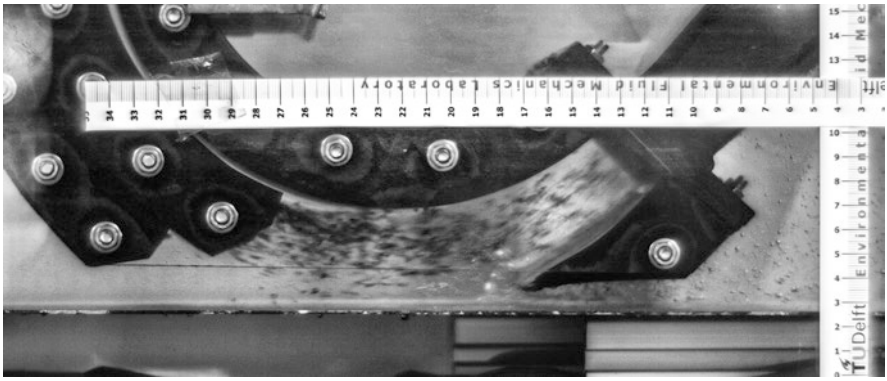

Fig. 7.4 Image obtained by a high-speed camera illustrating the flow direction including spilling water (highlighted by the presence of air bubbles) when the collector was stationary ($v_f = 0$). (Alhaddad & Helmons, 2023)

environmental impact of deep-sea mining activities, it is crucial to predict the evolution and fate of these plumes. This requires an understanding of the characteristics of the sediment-water mixture discharged from the collector. One key parameter of this discharge is the sediment concentration, which is influenced by the depth of the sediment layer picked up by the collector during operation. Therefore, gaining a thorough understanding of the interaction between Coandă-effect-based collectors and the ocean floor is essential to develop a collector with minimal environmental impact. To this end, Alhaddad and Helmons (2023) conducted a series of small-scale experiments to explore sand erosion caused by a Coandă-effect-based collector driving over a subaqueous sand bed in a water flume. Various operational conditions were explored, resulting in a set of quantitative data on sediment erosion associated with this type of collector. Their study showed that the Coandă-effect-based collector does not erode sediments primarily through flow-induced shear stress. Instead, the collector's water jet strikes the sediment bed at an inclined angle, leading to the collapse of the sediment layer. The majority of the collapsing sediment is transported with the deflecting flow into the collection duct, while the remaining portion is transported behind the collector head by the spilling water (see Fig. 7.4). The latter portion generates a sediment plume behind the collector, which brings about an additional environmental pressure besides the plume formed at the collector rear.

2.1 Operational Parameters

The key parameters controlling the pick-up efficiency of the collector in question are jet velocity v_j, collector's forward velocity v_f, and bottom clearance c (see Fig. 7.3). In the following, we will discuss the effect of these parameters on nodule

pick-up efficiency and sediment erosion depth. The former is defined as the ratio between the mass of collected nodules and the mass of nodules that are available for collection, while the latter is the thickness of the sediment layer collected by the collector.

2.1.1 Jet Velocity

Results of full-scale tests conducted by Alhaddad et al. (2023) showed that higher jet velocities result in higher pick-up efficiencies. This is attributed to the fact that higher jet velocities lead to larger pressure gradients under the collector (see Fig. 7.5 left), consequently dislodging more nodules from the sediment bed. Additionally, a higher jet velocity results in more water entrainment, which enhances the pressure difference under the collector, increasing the pick-up efficiency.

On the other hand, when jet velocities are higher, they cause greater erosion depths due to the increase in the impinging force of the flow onto the sediment bed. Experimental results of Alhaddad and Helmons (2023) showed a strong logarithmic correlation between the erosion depth and the impinging force exerted by the flow onto the sediment bed (see Fig. 7.6).

2.1.2 Collector's Forward Velocity

Alhaddad et al. (2023) tested only two forward velocities, where the higher forward velocity led to a lower pick-up efficiency despite the higher pressure gradient under the collector (see Fig. 7.5, middle). This is because a lower forward velocity allows more time for the nodules to respond to the pressure gradient and be picked up. This implies that a higher pressure gradient under the collector does not always lead to a higher pick-up efficiency. In other words, the collection process is highly dependent on the available time for the nodules to respond to the pressure gradient; if this time is insufficient, even an adequate pressure gradient will fail to pick up the nodules.

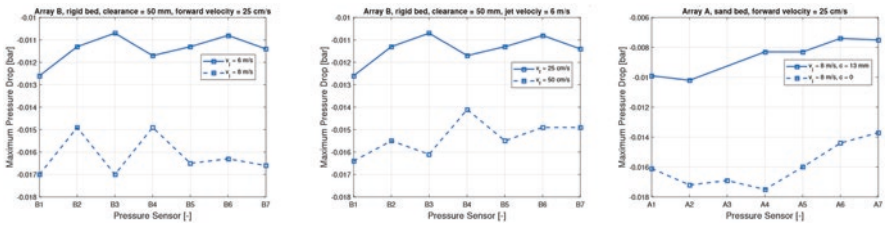

Fig. 7.5 Experimental results illustrating the effect of the jet velocity v_j (left), the forward velocity v_f (middle), and clearance c (right) on the maximum pressure drop under a Coandă-effect-based collector (Alhaddad et al., 2023). Pressure sensors B1-B7 and A1-A7 are spaced by a distance of 10 cm

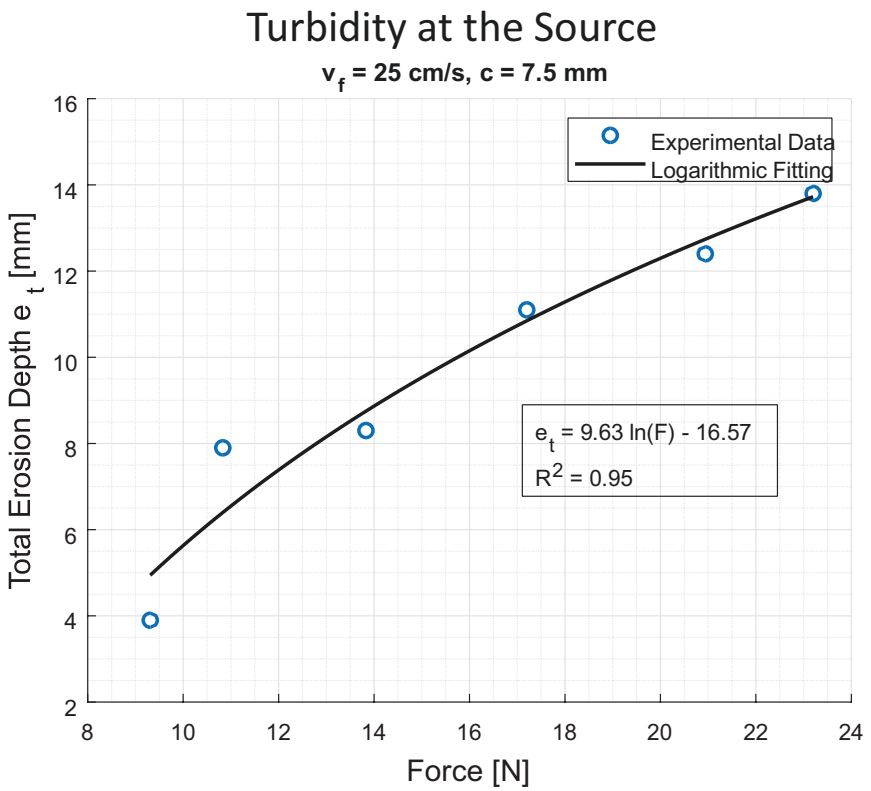

Fig. 7.6 Experimental results demonstrating a logarithmic correlation between the flow impinging force F and total erosion depth of sand e_t (Alhaddad & Helmons, 2023)

The sediment erosion process is significantly affected by the forward velocity, v_f, of the collector. Unsurprisingly, the experimental results of Alhaddad and Helmons (2023) clearly show that a lower v_f results in a greater erosion depth. This correlation is expected because a lower v_f exposes the sediment bed to the water flow for a longer period, resulting in the erosion of a thicker layer of sediment.

2.1.3 Bottom Clearance

The clearance under the rear cowl of the collection duct is another parameter that significantly affects the collection process. A smaller clearance results in a higher pick-up efficiency, reaching 100%, because it generates a greater suction force (see Fig. 7.5, right). Additionally, a smaller clearance implies that the centre of gravity of the nodules is closer to the underside of the collector, further increasing the pick-up efficiency.

In relation to sediment erosion, reducing the bottom clearance leads to a greater erosion depth, which is a logical correlation; when the underside of the collector is closer to the sand bed, a larger sand layer is exposed to the water flow, resulting in an increased erosion depth. To avoid the impingement of the flow onto the sediment bed, the bottom clearance should be increased above a certain threshold, which depends on the jet velocity and the forward velocity. However, this might result in a very low pick-up efficiency or even no nodule pick-up at all.

2.2 Discussion

In addition to pick-up efficiency, nodule collectors are also evaluated based on their environmental impact, which is a crucial performance metric. In the light of the findings described above, one can infer that if adjusting a certain operational parameter is favourable for the pick-up efficiency, it is mostly unfavourable from an environmental point of view (i.e. sediment erosion increases). This implies that the operational conditions of the collector need to be optimised to achieve the optimal pick-up efficiency and least environmental impact.

To gain further insights into the sediment erosion generated by the collector in question, a series of laboratory experiments, in which the collector drives along a cohesive sediment bed will be executed soon at Delft University of Technology.

3 Near Bed Release of Return Water Flow

The collection and separation stages of deep-sea mining will likely result in a large amount of process water that contains various types of fine sediments. Transporting this water to the surface for cleaning by filtration or hydrocyclones would presumably result in an unfeasible business case. For this reason, it is important to develop efficient strategies to return this process water in a controlled way that minimizes the impact both on the water column and the seabed. The key question is at which location in the water column should one release this water? High in the water column, to shorten the vertical transport distance of the return flow, would be economically attractive. On the other hand, this would affect a large volume of ambient water and could easily result in dispersion way beyond the designated mining area due to barotropic and baroclinic effects. For that reason it is also important to consider the release of process water in the proximity of the seabed, where the sediment was collected in the first place, and some degree of disturbance is unavoidable anyway by the act of mining vehicles for collection or excavation.

The challenge is then to let the sediment settle close to the impingement point and prevent the formation of turbidity currents that possibly extend outside the designated mining area. For this reason, it is important to understand the dynamics of sediment-laden flows close to the impingement point. Fig. 7.7 gives an overview of

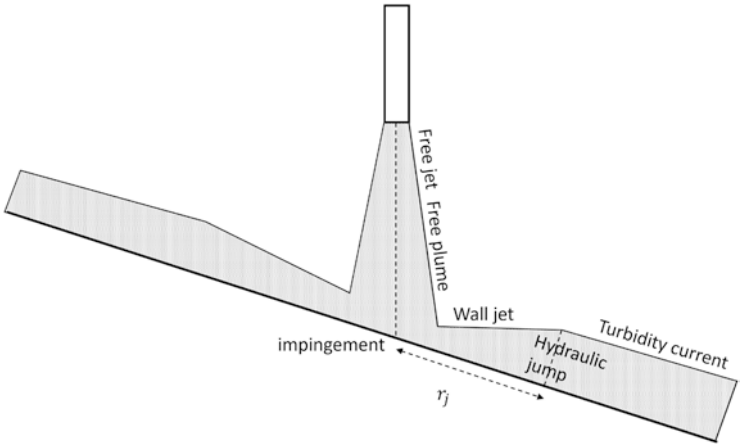

Fig. 7.7 Three different regions of mining return flow: free jet/plume region, impinging region, and turbidity current region

the different regions. Initially, the flow is controlled by the momentum flux from the nozzle; this is called the free jet region. At some point, the flow dynamics can be characterized as a free plume, and the flow can further accelerate by (negative) buoyancy associated with the sediment load. After impinging the plate the flow turns in a parallel direction relative to the seabed. The flow in this region can be described as wall-jet like (Chowdhury & Testik, 2015). After the formation of an internal hydraulic jump, a gravity (turbidity/density) current develops.

This section presents an experimental exploration of this problem and identification of scientific challenges in the prediction of the underlying near-bed sediment transport processes.

3.1 Experimental Exploration

Figure 7.8 shows the experimental set-up to explore the effect of impinging return flows Grunsven et al. (2018). The set-up consists of a large tank of 5 × 2 × 2 m and a 1 × 1 × 1 m mixing tank to prepare the jet mixture. A table is positioned inside the large flume chamber. The tabletop is mounted at 0.5 m from the flume floor. The advantage of this approach is that it limits side effects from the flume side walls as the density current tends to drop from the table and fill the volume below the tabletop. A second table with an inclined top (30°) was also available in order to study the effect of an inclined sea-bed slop on the development of the turbidity current. Light panels from the sides and mounted inside the table top helped to visualize the plume and turbidity currents. Concentrations and velocities are measured using ADV, and at several locations at the table top samples are taken to measure the local concentration. The stand-off distance H, concentrations, and discharge rate are

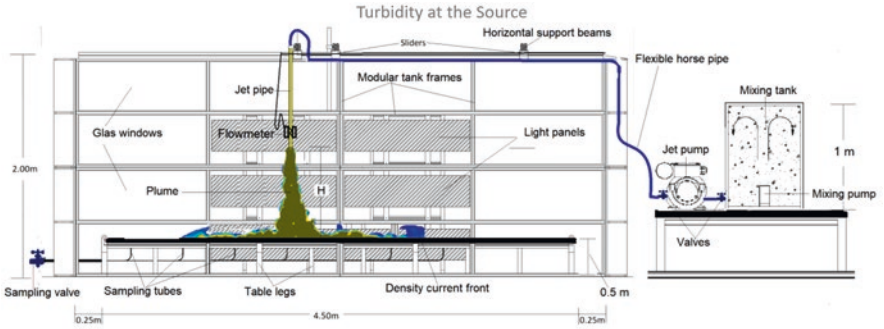

Fig. 7.8 Experimental set-up of the dredging engineering group of Delft University of Technology

Fig. 7.9 Impression of impinging return flow on inclined floor

variable. The sediment type was Millisil silica flour (or quartz powder) with a D_{10} = 15μm, d_{50} = 36μm and D_{90} = 70μm. Figure 7.9 provides an impression of a typical impingement on an inclined floor. In the experiments, sediment deposition rings form around the impingement point and exhibit complex dynamical behaviour (see Fig. 7.10). Based on the diameter and height of these rings in the order of 10–20 cm and 1–2 cm, respectively at the end of the experiments (10 min) the total amount of sediment that is deposited during the experiments is found to be significant, i.e. 50–90% of the sediment flux from the nozzle. It is very interesting to note that even in this simple case of a smooth wall, such complex morphological patterns emerge.

To obtain some understanding of this formation process, it is helpful to analyse the vertical profiles of the radial velocity at various distances from the impingement points (see Fig. 7.11). Close to the impingement point, the velocity profile shows a sharp maximum and turns into a more gradual profile when moving to a location further downstream of the impingement point. Also the turbulent kinetic energy profile collapses, which indicates that it becomes more difficult to keep sediment

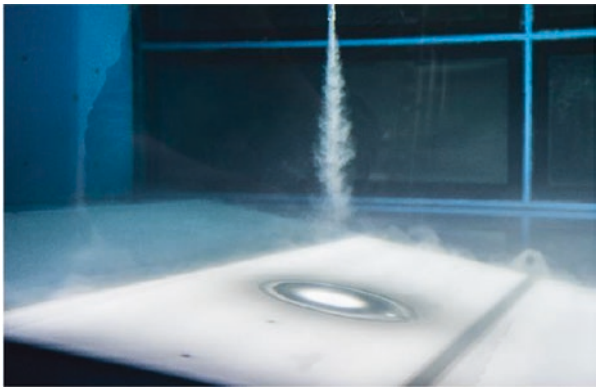

Fig. 7.10 Formation of a sediment deposition ring around the impingement point

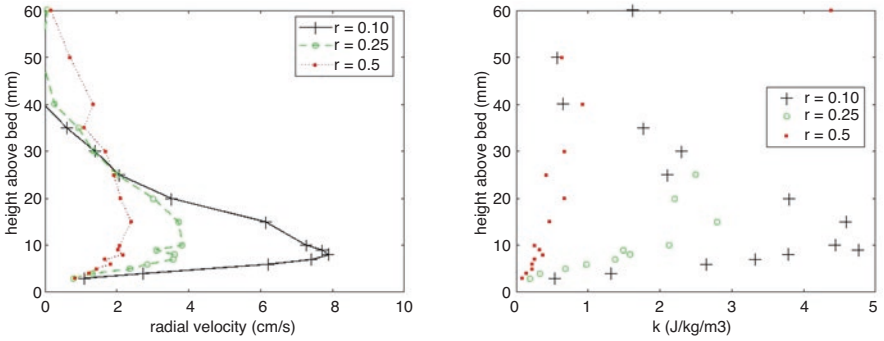

Fig. 7.11 Velocity and turbulent kinetic energy density versus height above the bed at three different radial distances r from the impingement point for the case with a stand-off distance of $H = 50$ cm, nozzle diameter 0.01 cm, and suspended sediment concentration of 20 g/l impinging on a horizontal table. Deposition rings were visible between $v_j r = 0.075$ m and $r = 0.15$ m in this experiment

suspended further downstream. Figure 7.12 shows the measured concentrations obtained with the draining systems that were mounted on the tabletop. It is seen that the sediment concentration quickly drops outside the range where the deposition rings were formed. From the velocity profiles in Fig. 7.11 at a location in this range, $r = 0.1$, and beyond this range, $r = 0.25$, it can be deduced that dilution by entrainment with ambient water is limited. The concentration mainly drops due to sediment deposition in the ring area. For $r > 0.25$, dilution by entrainment and removal of particles by settling further reduce the concentration.

In conclusion, this phenomenon is a subtle interplay between the flow in the impingement region and the turbidity current region, as indicated in Fig. 7.7. In the internal hydraulic jump that separates the wall jet region and the turbidity current region, turbulent and mean kinetic energy are strongly dissipated, which lowers the sediment carrying capacity further downstream of the jump. As a result, sediment is

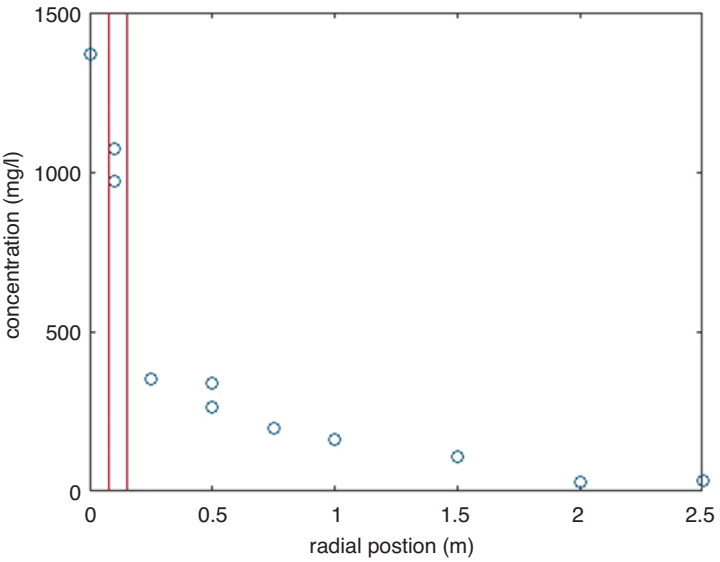

Fig. 7.12 Concentrations measured by the water tapping system versus the radial distance r from the impingement point for the case with a stand-off distance of $H = 50$ cm, nozzle diameter 0.01 cm and suspended sediment concentration of 20 g/l, impinging on a horizontal table. Deposition rings were visible between $r = 0.075$ m and $r = 0.15$ m in this experiment (indicated by the red vertical lines)

released from the flow and starts to form a deposition ring. In the experiments, the Shields parameter in the wall-jet region is presumably larger than the critical Shields parameter required for the initiation of motion of sediment on a smooth surface. In reality, particles that were already present on the sea bed could also be mobilized by the impinging flow, which would eventually result in a scour pit formation. At present, it is beyond the state-of-the-art of (numerical) models to describe these patterns satisfactorily. Therefore, further experimental study is required at both the laboratory and prototype scales to acquire a better understanding of the impingement process of sediment-laden return flows into the seabed. Also, high-resolution direct numerical simulations and Eulerian-Eulerian models could be helpful to further unravel the sediment transport physics near the impingement point.

4 Collector Plume Concept

The water-sediment mixture discharged from the back of the collector undergoes three distinct regimes: jet, plume, and turbidity current (Elerian et al., 2021). It is important to note that whether the flow is in the jet or plume phase depends on discharge parameters such as velocity and concentration. If the flow is

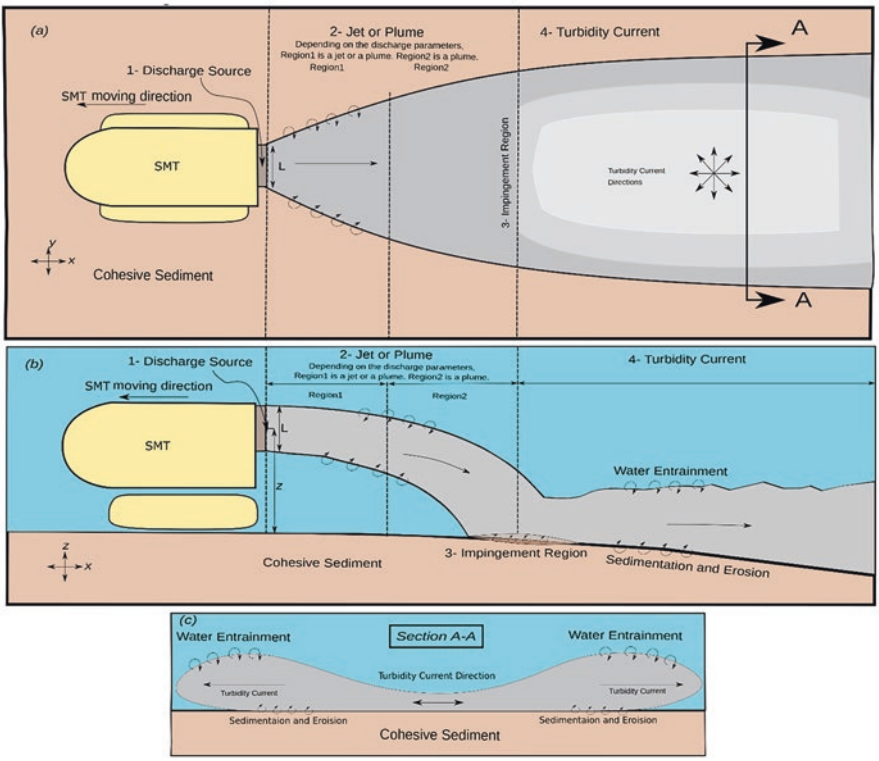

Fig. 7.13 Conceptual sketch of the evolution of the sediment-water mixture discharged by the SMT. (**a**) Top view of the collector plume, (**b**) side view of the collector plume, and (**c**) cross-section A-A indicating the sideways propagating turbidity current, after. (Elerian et al., 2022)

momentum-dominated, it is considered a jet, while if it is buoyancy-dominated, it is considered a plume. Once the mixture enters the plume phase, the density difference dominates the flow, and the mixture eventually reaches the seabed in a region known as the impingement region. At this point, the turbidity current begins to form, and a sideways propagating turbidity currents develop almost perpendicular to the direction of the collector movement (see Fig. 7.13).

The sideways turbidity current propagates due to the density difference between the denser water-sediment mixture and the lighter ambient fluid. Studying turbidity currents in the field is challenging due to the high cost of field experiments. However, scaled laboratory experiments are a widely used alternative for investigating such currents.

In this section, the study will primarily focus on the sideways propagating behaviour of turbidity currents in the near-field region, as these currents exhibit the longest time and length scales among the mixture phases previously mentioned. The investigation is divided into two main sections, which encompass experimental and numerical modelling, respectively.

4.1 Experimental Modelling of Non-cohesive Sediments

To investigate the influence of the particle size experimentally, lock-exchange experiments were conducted in the dredging lab of Delft University of Technology to test different sediment types with varying particle sizes.

4.1.1 Lock Exchange Experiments

Lock-exchange experiments are a type of laboratory experiment used to study the behaviour of turbidity currents. In these experiments, a tank is divided into two compartments by a gate or barrier. One compartment is filled with a denser fluid, such as water-sediment mixture, while the other compartment is filled with a lighter fluid, such as clear water. The gate is then removed, allowing the two fluids to mix and form a turbidity current (Fig. 7.14a).

In our experiments, we tested three non-cohesive sediment types: Type 1 with a particle size range of d_p = 65 − 105μm, Type 2 with a particle size range of d_p = 4 − 60μm, and Type 3, which was a 50-50 mix (in mass) of Type 1 and Type 2. In addition, we tested different initial concentrations ranging from 0.1% to 3% volumetric concentration for each sediment type to investigate their influence on the propagation of the turbidity current.

We recorded videos of each experimental run using a high-speed camera. To analyse the concentration of the turbidity current, we used a newly developed pixel-concentration method that allows us to detect concentration maps at any time of the

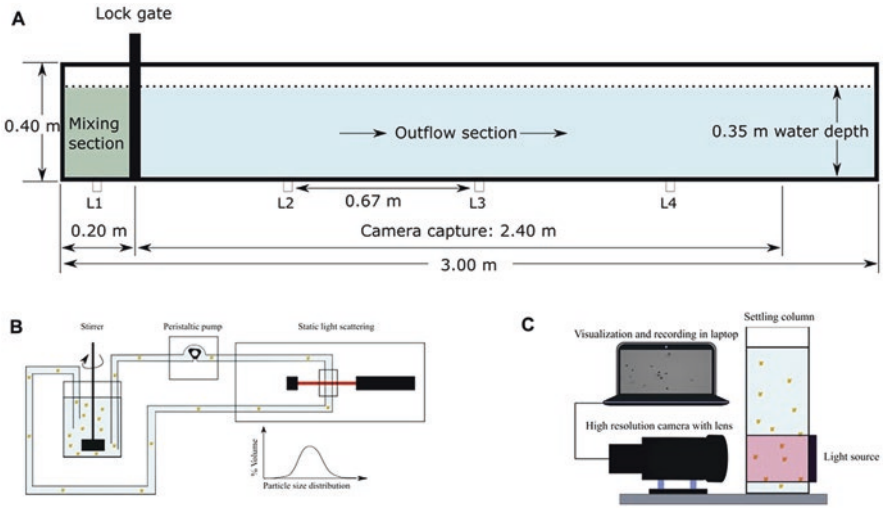

Fig. 7.14 Schematic representation of the set-ups: (Top) Lock exchange. The samples are taken at L1, L2, L3, and L4 locations. (Bottom left) Particle sizer. (Bottom right) FLOCCAM

entire turbidity current. Additionally, we were able to determine the forward velocity of the current from the recorded videos.

Based on the literature sources Rottman and Simpson (1983) and Huppert and Simpson (1980), it has been observed that a turbidity current in a lock-exchange experiment goes through three distinct phases based on its forward velocity: the slumping phase, the self-similar phase, and the viscous-buoyancy phase. The slumping phase occurs close to the lock gate, where the denser fluid near the lock collapses, leading to the formation of the turbidity current front or head. During this phase, the current propagates at a constant speed due to a balance between inertia and buoyancy forces. Subsequently, the self-similar phase begins, during which the propagation speed of the current is no longer constant and starts to decrease. Finally, the viscous-buoyancy phase takes over as viscous forces dominate the flow, causing the current to gradually diminish.

4.2 Findings

From these experiments, it was found that, increasing initial concentrations inside the lock yields high front velocities independent of sediment type, meaning that the transition time to the self-similar phase increases when increasing the initial concentration. Furthermore, increasing particle size leads to low front velocities, with coarse particle, lower-concentration currents transitioning to the self-similar phase more quickly than fine-particle currents, which take much longer to transition. Increasing initial concentrations neutralizes the particle size effect on current propagation. With higher-concentration currents, coarse particles have little to no effect on the motion of the current compared to fine-particle currents with the same initial concentration, while in lower-concentration currents, coarse particles settle and affect the forward velocity of the current. In the case of finer-particle, lower-concentration currents, low local concentration distribution values were observed.

For a more comprehensive understanding of these experiments, including the associated results and analysis, it is recommended that the reader read the work of Elerian et al. (2022).

5 Effect of Flocculation on Sediment Dispersion

Particle size distribution (PSD) controls how far deep-sea sediment plumes spread (Gillard et al., 2019; Spearman et al., 2020). Since aggregated particles (flocs) settle quicker than individual (unflocculated) particles of smaller size, flocculation can limit plume dispersion (Manning & Dyer, 2002; Spearman et al., 2019, 2020; Smith & Friedrichs, 2011; Gillard, 2019). The turbulence caused by mining vehicles, particularly in their vicinity, leads to rapid flocculation. Moreover, based on numerical findings, the aggregation mechanism was determined to be more dominant than the

break-up mechanism. As discussed by Gillard (2019), experiments on aggregation behaviour under various turbulent conditions and plume concentrations should reveal the likelihood of their deposition in the near-field area. Aside from that study, a few other publications present the hydrodynamic behaviour of original plume particles and model the impact scale at various temporal and spatial scales in the benthic boundary layer (Aleynik et al., 2017; Jones et al., 2017). The physical and chemical parameters of bottom sediments, the hydrodynamic regime (near and far field), bottom topography, and mining equipment type must be considered for this endeavour. Plume modelling of small-scale benthic impact experiments (discharge of approximately 10 kgs^{-1} along predefined tracks) showed that 90% of the suspended particles created by artificial seafloor disturbance settled within 2 km of the disturbance area (Fukushima, 1995; Nakata et al., 1997; Haalboom et al., 2022). Recent modelling of an industrial-scale, near-bottom sediment plume in the CCZ case study area with a discharge rate of 280 kg s^{-1} showed that more than 50% of suspended particles would settle within a few kilometers of the source region within 10 days. The remaining particles left the near-field area (Aleynik et al., 2017). The cohesive characteristics, aggregation potential, and settling processes of fine-grained deep-sea sediments, which affect plume sediment deposition, were, however ignored. Site-specific particle behaviour under varied plume concentrations and high-resolution bathymetric and oceanographic data are however essential to initialize and calibrate sediment transport models for the exploitation of nodule fields, where size, density, settling velocities, and strength of flocs over time are influenced by the properties of the suspending medium (salinity, organic matter content, sediment concentration, hydrodynamics) (Manning & Dyer, 2002; Mietta et al., 2009; Smith & Friedrichs, 2011; Chassagne, 2020). The deep-sea environment is, in principle, favourable for flocculation because of its high salinity and concentration of organic matter (Mewes et al., 2014; ISA, 2015; Volz et al., 2018). Flocculation has been shown to occur at very short timescales in natural environments in the presence of (microscopic) organic matter (Deng et al., 2019; Safar et al., 2019). The aim of the present work is to quantify how much flocculation can influence a plume's propagation and how the main characteristics (size, density) of the particles composing the plume evolve as function of run-out length. Two different approaches are investigated, one with artificial sediments and synthetic flocculants and one with original sediments from the Clarion Clipperton Zone.

5.1 Approach 1, Artificial Sediments

5.2 Materials and Methods

5.2.1 Clays

As illite is one of the dominant clays found in the top layer of the Clarion Clipperton Zone (CCZ) sediment where Deep Sea Mining (DSM) is performed (ISA, 2015), it was chosen for the initial experiments.

For further experiments, a lab-made artificial clay with a composition similar to CCZ clay was used and named "Artificial CCZ" (aka ACCZ). More information about the clays can be found in (Enthoven, 2021; Ali et al., 2022).

5.2.2 Flocculant

Organic matter found in the deep-sea region is expected to be the flocculating agent for the sediment plume (Jones et al., 2017; Gillard et al., 2019; Spearman et al., 2020; Jones et al., 2021). This organic matter is expected to be composed of parts of polyssacharides, and therefore, as was done in previous studies (Shakeel et al., 2020), an anionic polyacrylamide, referenced Zetag 4110 (BASF company) of medium anionic charge with high molecular weight, was used as a proxy for organic matter content.

5.2.3 Lock Exchange Set-Up

Lock exchange experiments were done in fresh as well as saline water. The saline water was produced by mixing 10 mM of $CaCl_2$ with freshwater. Three clay concentrations were used (10, 30, and 100 g/L), 30 g/L and 100 g/L with illite, and two different concentrations with ACCZ (10 g/L) and 30 g/L. Two flocculant dosages (0.25 mg/g and 0.75 mg/g) were also used. The dry clay was mixed with water in the lock exchange's mixing section for an hour before the lock gate was opened. This mixing made sure that homogeneous suspensions with a well-defined mean particle size could be obtained. In experiments with flocculant, the anionic polyelectrolyte was added and stirred for 30 s before the opening of the lock. The plume propagation was recorded with the help of a high-resolution camera. The videos were obtained with a Navitar 17mm lens on an IL5HM8512D: Fastec high-speed camera. The camera was placed 4.75 m from the lens to the front wall of the tank, and recording speed was 130 frames per second. The camera captured the 2.40 metres to the left of the lock. The camera and tank were placed beneath a black fabric to block out most of the light from outside. Samples were collected from four locations (L1, L2, L3, and L4 in Fig. 7.14 at the top) at the end of the experiments.

5.2.4 Particle/Flocs Size Distribution

Particle Size Distribution (PSD) analysis was conducted on the obtained samples using a Malvern master sizer 2000 (Fig. 7.14 bottom left), a technique based on static light scattering (SLS). With this set-up, within a few seconds a full PSD can be recorded.

5.2.5 Floc Settling Analysis

The FLOCCAM device records, using video microscopy, the settling velocity and size of particles. It was used to estimate PSD's (above 20 microns in size) and settling velocities of the different collected samples (Shakeel et al., 2021; Ye et al., 2020; Manning et al., 2007; Mietta et al., 2009). Figure 7.14 bottom right gives a schematic representation of the equipment. The size, shape, and settling velocity of the flocs are calculated from the videos using the software package Safas (MacIver, 2019).

5.3 Results

There is no substantial difference between experiments conducted in fresh and saltwater, both for illite and for ACCZ sediment when no flocculant is used. The results for 30 g/L clay are given in Fig. 7.15 Regardless of the clay concentration in either fresh and saltwater, the sediment plumes reached the lock exchange's end in those experiments. The plume head velocity scales with the square root of the plume density, as expected (Huppert, 2006). As salt-induced flocculation is slow, with flocculation times of the order of 15–30 min even under ideal shear circumstances (Mietta, 2010). It is expected that no significant effect was seen over the experimental period of the current study (less than 1 min).

When experiments with added flocculant were performed, the distance travelled in saltwater experiments for all clay types and concentrations was reduced considerably, and the sediment plumes did not reach the end of the lock exchange. In Fig. 7.16 results for 0.75 mg/g flocculant are given. The results using 0.25 mg/g flocculant can be found in (Enthoven, 2021; Ali et al., 2022), but the general observations remain the same. For the experiment done in freshwater with flocculant, the sediment plume reached the end of the lock exchange (100 g/L) or nearly half of the

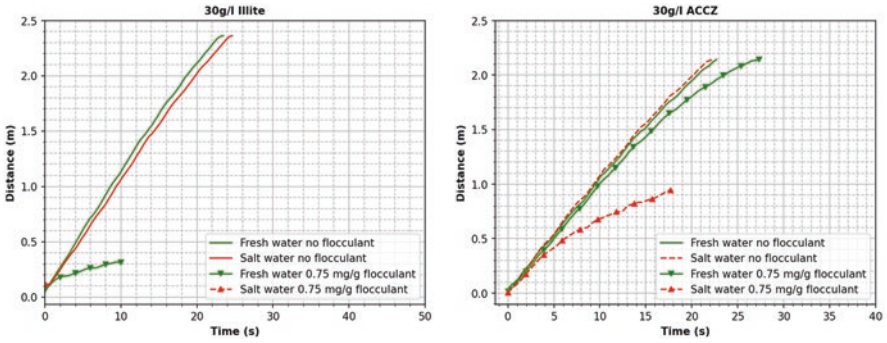

Fig. 7.15 Head propagation as a function of time for 30 g/L illite and ACCZ in different suspending media (indicated in the legends)

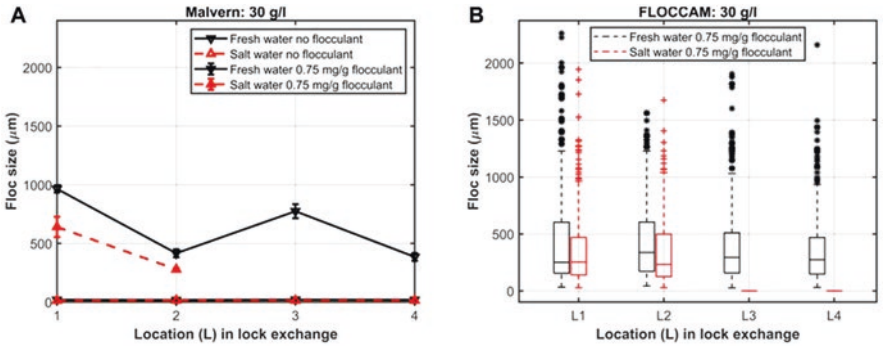

Fig. 7.16 Hydrodynamic size of ACCZ flocs at locations L1-L4 in the lock exchange. (**a**) Results obtained by SLS and (**b**) results obtained from FLOCCAM

lock exchange (10 g/L). The weak flocculation in freshwater accounts for this difference between fresh and saline water experiments. Freshwater contains enough cations to promote slight flocculation between the negatively charged clay and flocculant (Ibanez Sanz, 2018). The cation concentration in saltwater hugely promotes flocculation, because the cation chosen (Ca^{2+}) is divalent (Shakeel et al., 2020; Chassagne, 2020). For 100 g/L experiment with illite, it was found that the system did not properly flocculate and in all cases the sediment plumes reached the end of the lock with the same speed.

5.3.1 Mean Floc Size as Function of Travel Distance

Figure 7.16 displays the mean floc size of the samples taken at the various locations L1-L4. No flocculation was found to happen without the flocculant in both fresh and saltwater, as for each location, the mean particle size was found to be equal to the mean clay size. For both experiments with illite, the mean particle size was found to be around 5 microns at all locations, whereas for experiments with ACCZ, it was found to be between 12 and 20 microns. These sizes are in line with the sizes found using SLS (5 and 10–20 microns respectively). The bars given in the left figures (measured by SLS, using a Malvern ParticleSizer) represent the standard deviation around the mean floc size, whereas in the right figures (measured by video microscopy, using the FLOCCAM) the box plot represents the median particle sizes with interquartile range and outliers.

It was observed that freshwater flocs were larger than saltwater flocs in the presence of organic flocculant. Because of the electrostatic repulsion between the charged groups on the polymeric flocculant, the flocculant in freshwater is expected to be less coiled in fresh compared to saltwater. As a result of shearing during propagation, it is observed that in saltwater the size of flocs created with illite clay is reducing as function of travel distance. This difference is not observed for the ACCZ clay.

5.3.2 Settling Velocity Distributions as Function of Size and Travel Distance

Figure 7.17 displays the settling velocities and particle size ranges for 30 g/L ACCZ with 0.75 mg/g of flocculant at sites L1 and L4 (for freshwater). The settling velocities in freshwater are smaller than in saltwater at the point where the sediment plume settles down. This is due to the fact that the flocculant is less coiled in freshwater than in saltwater, leading to denser flocs with a faster settling velocity. This was confirmed by the video images. In the case of 30 g/L ACCZ, the settling behaviour and floc size for the saltwater sample did not change between L1 and L2, indicating that optimum flocculation has occurred in the mixing tank. The bridging between anionic polyelectrolyte and clay by saltwater cations is, in that case, complete. In contrast, the flocculation in the mixing tank for the freshwater sample is most probably incomplete due to the limited amount of cations. Observing the similarity between the distributions in location L1 for all experiments, the created flocs have the same features (same size, same settling velocity) as flocs formed in saltwater environments. Flocs, clay particles, and unbounded flocculant are released when the lock is opened. Freshwater containing cations comes into contact with the clay particles and unbounded flocculant. Because flocculation by polyelectrolytes is fast and of the order of seconds (Ibanez Sanz, 2018; Shakeel et al., 2020; Ali & Chassagne, 2022), these cations will act as a binding agent, inducing flocculation.

Several flocs formed during the propagation of the sediment plume in 30 g/L ACCZ experiment in freshwater are observed to be elongated, resulting in flocs with large equivalent diameters (shown by the red circle in the bottom panels of Fig. 7.17). These big flocs have a very slow settling velocity because they are formed of low-density uncoiled flocculant connected to some clay. These flocs were unable to

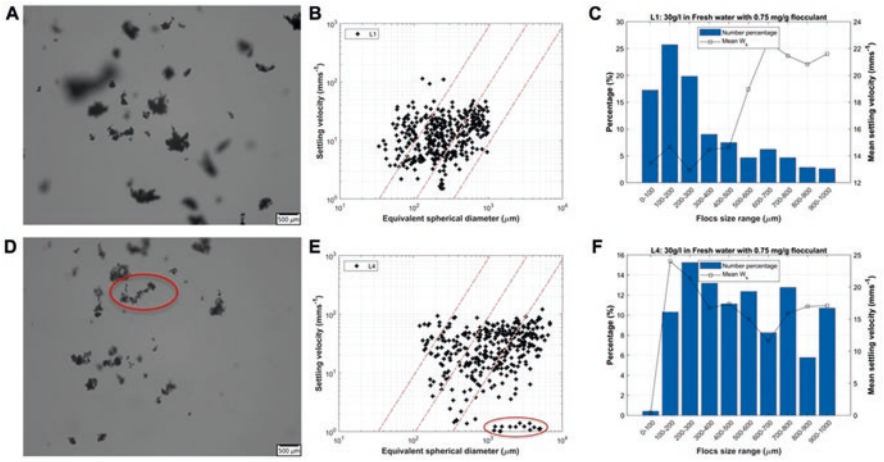

Fig. 7.17 (**a**, **d**): Snapshots of the videos; (**b**, **e**): Settling velocity and particle size analysis of the 30 g/L ACCZ with 0.75 mg/g flocculant in fresh water collected at L1 and L4. The dashed lines in (B, E) represent the effective density lines from left to right: 1600, 160 and 16 kgm^{-3}

catch more clay particles or coils due to their limited residence period in the water column. Coiling of flocs happens over longer periods of time when turbulent shear causes the polyelectrolyte's loose ends to collapse onto the floc. The flocs get rounder and denser as a result (Shakeel et al., 2020).

5.4 Approach 2, Original Sediments

Oceanographic data and surface sediment samples were collected using a multicorers at different locations in the eastern sectors of the CCZ, where flat abyssal plains, NW–SE trending ridge systems, and seamount rises produce fine-grained sediments at 4300 m. Roller tank, shear tank, and water column simulator incubations, as well as a settling tube, were used to analyse the particle behaviour of the sediment plumes under different turbulent conditions (Gillard, 2019). The dependence of the various concentrations of aggregated plume particles on the settling behaviour was investigated under in-situ temperature conditions for periods of 24 h. The particle size range covered original deep sea sediments which were released into the water column under high shear rates (a centrifugal pump simulating the exhaust plume behind a mining vehicle) to form large aggregates >2000 μm in size. These formed rapidly in the wake of the vehicle. For these analyses a LISTT – 100 X particle analyser and a particle camera set-up as described in (Gillard et al., 2022) were used. FIJI software (v.1.51n) was used to calculate aggregate size and shape descriptor parameters (circularity, roundness, and solidity) as described by (Shen, 2016). For mesocosm experiments visualizing the generation of fluid muds and subsequent consolidation of aggregated plume sediments, the surface sediments were dispersed using a centrifugal pump (7500 l/h) and subsequently transferred into a calibrated water column simulator (110 cm diameter, 1000 L), based on the design of (Sanford, 1997) and (Crawford & Sanford, 2001), thus allowing larger water volumes and avoiding constant shear as produced by Couette cylinders, which is intrinsically unrepresentative of natural turbulence (Arnott et al., 2021). Shear rates of 0.1 G to 1 G were simulated with such simulator. These represent flow conditions typical for slow deep sea bottom currents and elevated currents near the seafloor generated by passing eddies. Turbidity was determined using a Aquatech 310TY sensor.

5.5 Results

Median particle size (D50) of disaggregated surface sediments from three different sectors of the eastern CCFZ varied between 8 − 25μm. The average bulk wet density of these sediments was ≈1230 kgm^{-3} with a porosity of 87 %. Figure 7.18 presents the aggregation behaviour of two sediment plumes of different particle concentrations (1 g/L vs. 10 g/L) under two different turbulent conditions (0.1 G

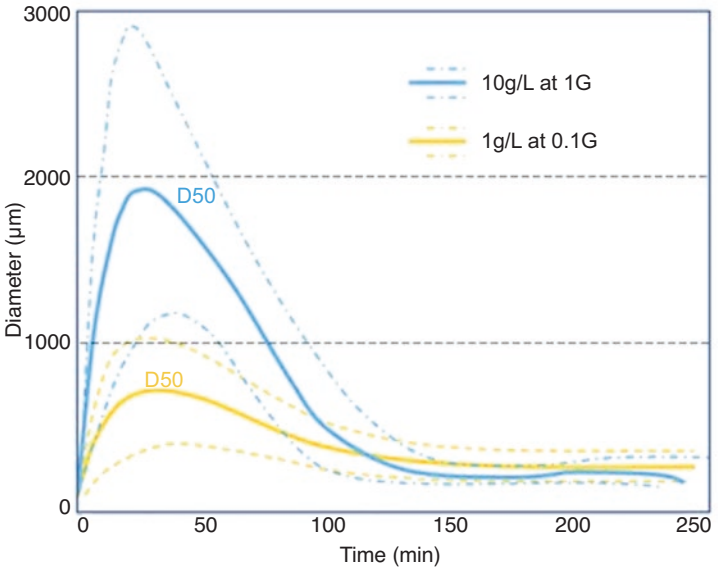

Fig. 7.18 Sediment plume aggregation dynamics in the water column simulator. d_{50} (solid lines ±STD (dashed lines) from particle camera data, analysed with Matlab

(0.1 s^{-1}, ≈ 4 cm/s flow velocity) vs. 1 G (1 s^{-1}, ≈15 cm/s flow velocity). The results show the expected spectrum of aggregate formation, from low shear/low particle concentration to high shear/high particle concentration. The results reveal that both hydrodynamic conditions result in a rapid formation of large particles within the first 30 min after release. During that time, the size distribution of primary particles of d_{50} of 8-25 µm rapidly shifts towards large aggregates with d_{50} of 700µm to almost 2000µm respectively while after 24 h particles of d_{50} of 300–400 µm still remain in suspension showing ongoing aggregation of the remaining particle loads. This would continue during a permanent release of a plume, while simultaneously these particles are settling (exported) towards the seafloor. Within the bottom boundary layer behind the mining vehicle, an export of ≈ 50 % of the initial plume concentration can be seen. After this initial phase of rapid aggregate formation and/or once the release stopped, the particle sizes decrease and smaller particles of lower settling velocities are formed which widen the general fallout area in downstream direction of the bottom currents or resulting gravity current. Most of the expelled particle mass will thus settle behind a moving mining vehicle with 1 h, thus focusing the main fallout area to a few km^2 around the exploration site. The results however also show that even after 24 h the turbidity is elevated with particle concentrations of a few mg/L and thus still one order of magnitude higher than background concentrations of ≈ 0.1 mg/L (Haalboom et al., 2023).

The settling velocities of aggregates during the first 120 min after release varied for the d_{50} size between ≈ 120 and 210 m/d under the low turbulence/low particle

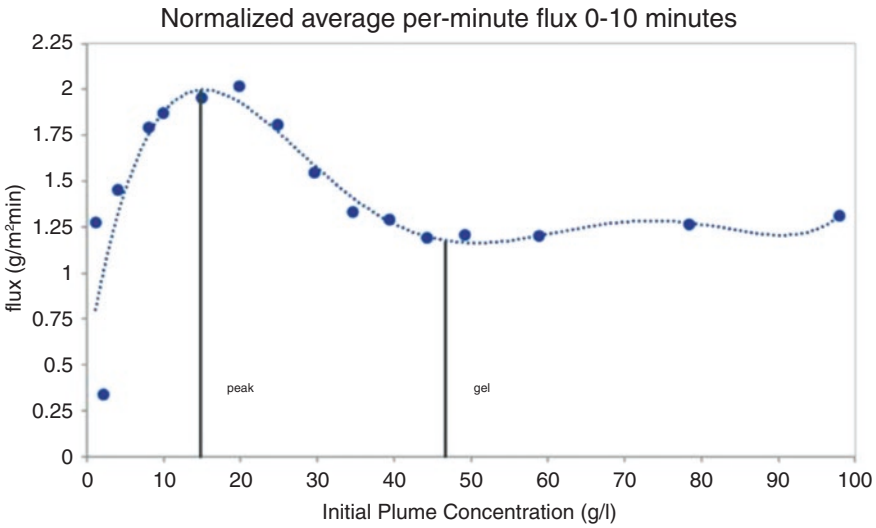

Fig. 7.19 Normalized average per-minute settling flux for CCZ sediment plume

concentration conditions and ≈ 420 to 700 m/d under the high turbulence/high particle concentration conditions. Under these conditions, 90 % of the flocs settle through a 1 m thick water column and form a fluid mud, which could be exported as gravity current. The results partly resemble the flocculation behaviour of artificial sediments and flocculants, as shown in Fig. 7.15.

The settling flux result for CCZ sediment plumes under varying particle concentrations is presented in Fig. 7.19 and should reveal the behaviour of aggregates under very high release concentrations behind the mining vehicle once settled into the fluid mud. Hindered settling is expected at particle concentrations of a few g/L (Mehta, 1986). CCZ sediment plumes behaved in three distinct modes that resembled the settling behaviour described by (Dankers & Winterwerp, 2007). Before the volumetric sediment concentration of the solids (Φ, after (Kynch, 1952) peaks at 15 g/L, the settling flux rises somehow linearly with increased sediment plume concentration. Beyond Φ_{peak}, the flux decreased showing the effect of hindered settling behaviour. Finally, the profile flattens out past Φ_{gel} (45 g/L) to a relatively constant per-minute flux, indicating that a gel-like suspension had formed at Φ_{gel}. This results in the formation of a fluid mud, which then slowly consolidates over many hours.

The experiments suggest that the fallout zones of particles behind a moving mining vehicle are relatively local. This will result in heavy blanketing of the sediments in the direct vicinity of an exploration site unless the fluid mud is carried away by a gravity current (Elerian et al., 2022). This was confirmed during the first in-situ collector test in 2021 in the CCFZ within the EU MiningImpact 2 project (Igazis et al, Nature, in review).

5.6 Findings

In this work, the influence of flocculation on turbidity currents was studied inside a lock exchange, where the current propagation time was of the same order of magnitude. It was shown that in the presence of an organic flocculating agent (anionic polyelectrolyte), flocculation was promoted. It was found that in both fresh and saltwater, flocs can be formed in a matter of seconds with the flocculant used in this study. As a result, the sediment plume was able to settle more quickly. The synthetic flocculant used is a proxy for organic matter found in marine environments (usually also negatively charged). It remains to be investigated if the type of flocculant has a significant impact on flocculation. This will be possible once the organic matter found in our area of interest (i.e. the Clarion-Clipperton Zone) has been fully characterized. The results presented in this article are generic and thus apply to a wide range of turbidity currents. We demonstrated that flocculation may occur even in freshwater, where flocculation is supposed to be difficult because of the electrostatic repulsion between organic matter and clay. This means that flocculation should be accounted for in turbidity current models. The obtained results demonstrate that flocculation is a relevant phenomenon that may already be contributing in the near field. Building experience with more conventional sediments allows us to better understand and design experiments with real CCZ sediment, which is the next step.

6 Numerical Modelling of Flocculation Effects in Near-Field

Given the time and cost-intensive nature of these experiments, it is crucial to utilize mathematical and numerical models to predict turbidity current behaviour with minimal computational effort. However, it is equally important to properly validate and calibrate these models.

6.1 The Mixture Model (Drift-flux Model)

The mixture model, which is also known as drift flux model, is a mathematical model used to describe the behaviour of multiphase flow, such as the flow of a mixture of sediment and water. In this context, each particle size fraction is considered a discrete phase, while the water is the continuous phase.

The drift-flux model treats turbidity currents as a single continuum, requiring a single momentum equation to be solved for the mixture as a whole. However, it takes into account the depositional behaviour of particles through the use of drift velocity. A clear mathematical structure for the drift-flux model is reported in detail in the work of Goeree (2018).

The multi-fraction drift-flux model was incorporated into the widely-used open-source computational fluid dynamics (CFD) software OpenFOAM. In addition, the blockMesh utility in OpenFOAM was used to generate a two-dimensional mesh that represents the lock-exchange tank. Furthermore, numerical experiments were conducted with the same initial conditions as the aforementioned experiments for the purpose of validating the newly implemented model. The measured forward velocity and concentration profiles from the experiments were compared to those obtained from the numerical simulations, revealing a high degree of agreement. This finding underscores the efficacy of the multi-fraction drift-flux model as a powerful tool for accurately predicting turbidity currents.

6.2 The Population Balance Equation (PBE)

The aforementioned multi-fraction drift-flux model has been demonstrated to be well-suited for simulating noncohesive sediment. However, the sediment in the deep sea exhibits cohesive properties in the presence of organic content. This cohesive nature allows the sediment to aggregate while in suspension, and in certain scenarios with high shear rates, the formed flocs may break up from each other. Recent research has increasingly recognized the crucial role of flocculation in deep-sea mining turbidity flows, as evidenced by studies such as those by Gillard et al. (2019), Spearman et al. (2020), Notably, Gillard et al. (2019) conducted a controlled laboratory experiment and revealed that under specific mixing conditions, the median particle size (d_{50}) of a Clarion Clipperton Fracture Zone (CCZ) sediment mixture can increase from 12 μm to 600 μm in just 7 min, indicating a rapid aggregation process among sediment particles.

The unique behaviour of cohesive sediment in suspension presents additional challenges and complexities that need to be considered in the development of accurate models for simulating turbidity currents in deep sea environments. Extensive efforts have been dedicated to the mathematical framework for describing the complex mechanisms of flocculation, resulting in the establishment of the Population Balance Equation (PBE) as a key tool in capturing the intricate dynamics of floc formation and evolution (Hounslow et al., 1988). Consequently, the multi-fraction drift-flux model was extended by incorporating the PBE to account for the aggregation and break-up processes. The six source terms of the PBE were added to the phase transport equation of the drift-flux model. The details of the coupling between the PBE and the drift-flux model are clearly reported in the work of Elerian et al. (2023) for further reference.

The aggregation of particles in shear-induced flows leads to an increase in floc size and a decrease in density, as water becomes trapped within the flocs during the aggregation process. This phenomenon directly affects the settling velocity of the flocs, which in turn impacts the accuracy of predictions for mixture hydrodynamics. To accurately account for these changes, an improved definition of settling velocity that considers both the primary particle size and the fractal dimension of the flocs is

used in the model. Furthermore, the most important parameters of the model, such as the fractal dimension, floc shape coefficient, and breakage coefficient were calibrated using the experimental work of Gillard et al. (2019).

6.3 Near-Field Modelling

Following the successful validation of the multi-fraction drift flux model and calibration of the Population Balance Equation (PBE) source terms, we have gained confidence to proceed with the near-field modelling, which focuses on the area approximately 100 m behind the collector. These simulations were conducted in order to distinguish the flocculation nature and its effect in the near-field region.

Numerical simulations were conducted for a distance of 100 m behind the collector, using a realistic discharge scenario. The collector velocity was set at 0.5 m/s, the discharge velocity at 0.5 m/s, the discharge volumetric concentration at 1%, the volumetric sediment flux at 0.01 m^2/s, and the volume flux at 1 m^3/s. The numerical simulation was run for 250 s to ensure a steady state situation for the propagation of the sideways propagating turbidity current. Two numerical runs were compared: one with flocculation, where the flocculation source terms were active, and the other without flocculation, where flocculation was not considered, modelling non-cohesive sediment.

The comparison between the two cases has revealed that sediment readily forms aggregates (see Fig. 7.20), which are larger particles that settle once the turbidity current subsides, likely occurring in the far-field region. The turbulence caused by

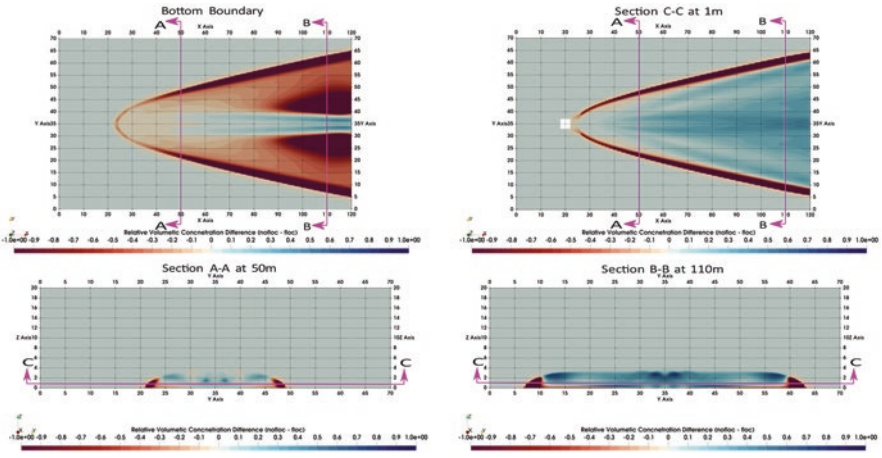

Fig. 7.20 Z and X normal sections show the relative differences between the flocculation and no-flocculation cases. The Z-normal sections are taken at the BOTTOM boundary (left) and 1 m from the bottom (right) which is section C-C, while the X-normal sections are taken at 50 m and 110 m from the INLET boundary

SMT, especially in the region close to the SMT, promotes rapid flocculation. Moreover, the aggregation mechanism was found to be more dominant than the break-up mechanism, based on the numerical findings. While the effects of flocculation can be observed in the near-field region, their significant impact on the turbidity current near the SMT is limited.

7 Conclusions

In this chapter, we have shown various essential results to allow for better prediction of sediment dispersion near the bed. Some insights have been provided into how the collector design of a Coandă-effect-based nodule collection system can influence the erosion of the seabed, differentiating between what sediment might be collected and what might be spilled into the near seabed environment, and whether and how sediment dispersion near the bed might be predicted.

The experimental explorations of the near-seabed release of SWOE open up the question of whether the formation of morphological structures could help to prevent the dispersion of sediments outside the designated mining area. The challenge is to dissipate the mean and turbulent kinetic energy of the flow and thereby reduce the sediment transport capacity of the flow. Design parameters that may influence the flow of the sediment plume will be the nozzle diameter, nozzle angle, stand-off distance, discharge rate, and discharge composition. In addition, the deposition of sediment could be promoted by using topological features or by altering the seabed, e.g creating morphological structures by the mining vehicles used for the collection process.

This kind of research should be conducted in-line with other attempts to promote the deposition rate, e.g. by flocculation.

The experiments conducted with cohesive sediments hint at several trends. Aggregation is likely to take place in the collector plume, increasing the sediment deposition rate and effectively reducing the driving mechanism of the sideways propagating turbidity currents. This means that flocculation should be accounted for in turbidity current models. The obtained results demonstrate that flocculation is a relevant phenomenon that may already be contributing in the near field. Building experience with more conventional sediments allows us to better understand the mechanisms at play. Experiments with real CCZ sediments are essential to providing quantitative information for these specific cases.

The multi-phase drift flux model for near field modelling of the collector plume shows some of the potential effects flocculation might have on the sediment composition (and thus settling velocities) already within the vicinity of the SMT. It is in this area where the design and operation of the equipment might be able to influence the collector plume release conditions, potentially improving overall settling velocities by optimizing mixing and sediment concentration. Further studies would be required to fully explore the design space available to identify under which conditions plume dispersion might be minimized. Obviously, this will only be possible

under the constraint of effective nodule pick-up, enabling a viable economic production.

Acknowledgements The results presented are part of the Blue Harvesting project, which is funded by the European Institute of Innovation and Technology, EIT Raw Materials under Project Agreement 18138, Specific Grant Agreement No. [EIT/RAW MATERIALS/SGA2019/1], TREASURE project (Towards Responsible ExtrAction of SUbmarine mineral REsources), which is financially supported by NWO-STW and PLUMEFLOC project, (TMW.BL.019.004, Topsector Water and Maritiem: Blauwe route) within the MUDNET academic network.

References

Aleynik, D., Inall, M., Dale, A., & Vink, A. (2017). Impact of remotely generated eddies on plume dispersion at abyssal mining sites in the Pacific. *Scientific Reports, 7*(1), 1–14, Springer US.

Alhaddad, S., & Helmons, R. (2023). Sediment erosion generated by a Coandă-effect-based polymetallic-nodule collector. *Journal of Marine Science and Engineering, 11*(2), 349.

Alhaddad, S., Mehta, D., & Helmons, R. (2023). Mining of deep-seabed nodules using a Coandă-effect-based collector. *Results in Engineering, 17*, 100852.

Ali, W., & Chassagne, C. (2022). *Comparison between two analytical models to study the flocculation of mineral clay by polyelectrolytes*. Manuscript submitted for publication.

Ali, W., Enthoven, D., Kirichek, A., Helmons, R., & Chassagne, C. (2022). Can flocculation reduce the dispersion of deep sea sediment plumes? In *Proceedings of the world dredging conference (WODCONXXIII), Copenhagen, Denmark*.

Arnott, R. N., Cherif, M., Bryant, L. D., & Wain, D. J. (2021). Artificially generated turbulence: A review of phycological nanocosm, microcosm, and mesocosm experiments. *Hydrobiologia, 848*, 961–991.

Atmanand, M., & Ramadass, G. (2017). Concepts of deep-sea mining technologies. In R. Sharma (Ed.), *Deep-Sea mining*. Springer.

Chassagne, C. (2020). *Introduction to colloid science*. Delft Academic Press. ISBN 9789065624376.

Chowdhury, M., & Testik, F. (2015). Axisymmetric underflows from impinging buoyant jets of dense cohesive particle-laden fluids. *Journal of Hydraulic Engineering, 141*(3), 04014079.

Crawford, S. M., & Sanford, L. P. (2001). Boundary shear velocities and fluxes in the MEERC experimental ecosystems. *Marine Ecology Progress Series, 210*, 1–12.

Dankers, P. J. T., & Winterwerp, J. C. (2007). Hindered settling of mud flocs: Theory and validation. *Continental Shelf Research, 27*(14), 1893–1907.

Deng, Z., He, Q., Safar, Z., & Chassagne, C. (2019). The role ofalgae in fine sedimentflocculation: In-situ andlaboratory measurements. *Marine Geology, 413*, 71–84.

Elerian, M., Alhaddad, S., Helmons, R., & Van Rhee, C. (2021). Near-field analysis of turbidity flows generated by polymetallic nodule mining tools. *Mining, 1*, 251–278. https://doi.org/10.3390/mining1030017

Elerian, M., van Rhee, C., & Helmons, R. (2022). Experimental and numerical modelling of Deep-Sea-mining-generated turbidity currents. *Minerals, 12*(5), 558.

Elerian, M., Ziyang, H., van Rhee, C., & Helmons, R. (2023). Flocculation effect on turbidity flows generated by deep-sea mining: A numerical study. *Ocean Engineering, 277*, 114250.

Enthoven, D. (2021). *Plume dispersion of low-density clayey suspension turbidity currents created by deep-sea mining* (Master thesis), Technische Universiteit Delft.

Fukushima, T. (1995). *Overview "Japan Deep-Sea impact experiment = JET". First ISOPE Ocean mining symposium*. International Society of Offshore and Polar Engineers.

Gillard, B. (2019). *Towards Deep Sea mining-impact of mining activities on benthic pelagic coupling in the clarion Clipperton fracture zone* (PhD thesis). Universität Bremen.

Gillard, B., Purkiani, K., Chatzievangelou, D., Vink, A., Iversen, M. H., & Thomsen, L. (2019). Physical and hydrodynamic properties of deep sea mining-generated, abyssal sediment plumes in the Clarion Clipperton Fracture Zone (eastern-central Pacific). *Elementa, 7*, 5.

Gillard, B., Harbour, R. P., Nowald, N., Thomsen, L., & Iversen, M. H. (2022). Vertical distribution of particulate matter in the clarion Clipperton zone (German sector)—Potential impacts from Deep-Sea mining discharge in the water column. *Frontiers in Marine Science, 9*, 820749.

Gillham, J. (2022). Economically viable selective harvesting of polymetallic nodules. In *Proceedings of the 50th underwater mining conference, St. Petersburg, Florida, USA*.

Goeree, J. (2018). *Drift-flux modeling of hyper-concentrated solid-liquid flows in dredging applications* (PhD thesis). Delft University of Technology.

Grunsven, F., Keetels, G., & Van Rhee, C. (2018). The initial spreading of turbidity plumes—Dedicated laboratory experiments for model validation. In *Proceedings of the 47th underwater minerals conference, Bergen, Norway*.

Haalboom, S., Schoening, T., Urban, P., Gazis, I.-Z., de Stigter, H., Gillard, B., Baeye, M., Hollstein, M., Purkiani, K., Reichart, G.-J., Thomsen, L., Haeckel, M., Vink, A., & Greinert, J. (2022). Monitoring of Antrhopogeneic sediment plumes in the clarion-Clipperton zone, NE equatorial Pacific Ocean. *Frontiers in Marine Science, 9*, 699.

Haalboom, S., de Stigter, H., Mohn, C., Vandorpe, T., Smit, M., de Jonge, L., & Reichart, G.-J. (2023). Monitoring of a sediment plume produced by a deep-sea mining test in shallow water, Malaga Bight, Alboran Sea (southwestern Mediterranean Sea). *Marine Geology, 456*, 106971.

Hong, S., Choi, J.-S., Kim, J.-H., & Yang, C.-K. (1999). Experimental study on hydraulic performance of hybrid pick-up device of manganese nodule collector. In *Proceedings of the third ISOPE Ocean mining symposium*.

Hong, S., Kim, H.-W., Yeu, T., Choi, J.-S., Lee, T., & Lee, J.-K. (2019). Technologies for safe and sustainable mining of deep-sea minerals. In R. Sharma (Ed.), *Environmental issues of deep=sea mining: Impacts, consequences and policy* (pp. 95–143).

Hounslow, M., Ryall, R., & Marshall, V. (1988). A discretized population balance for nucleation, growth, and aggregation. *AICHE Journal, 34*(11), 1821–1832.

Huppert, H. E. (2006). Gravity currents: A personal perspective. *Journal of Fluid Mechanics, 554*(1), 299–322. https://doi.org/10.1017/s002211200600930x

Huppert, H., & Simpson, J. (1980). The slumping of gravity currents. *Journal of Fluid Mechanics, 99*(4), 785–799.

Ibanez Sanz, M. (2018). *Flocculation and consolidation of cohesive sediments under the influence of coagulant and flocculant* (PhD thesis). Delft University of Technology.

ISA. (2015). *A geological model of polymetallic nodule deposits in the clarion-clipperton fracture zone*. [WWW Document], Technical report 6. ISA 2019. Current status of the reserved areas with the international seabed authority. [WWW Document], Technical report.

Jones, D. O. B., Kaiser, S., Sweetman, A. K., Smith, C. R., Menot, L., Vink, A., Trueblood, D., Greinert, J., Billett, D. S. M., Arbizu, P. M., Radziejewska, T., Singh, R., Ingole, B., Durden, J. M., Clark, M. R., Stratmann, T., & Simon-lledo, E. (2017). Biological responses to disturbance from simulated deep-sea polymetallic nodule mining. *PLoS One, 12*(2), e0171750.

Jones, D. O. B., Simon-Lledó, E., Amon, D. J., Bett, B. J., Caulle, C., Clément, L., Connelly, D. P., Dahlgren, T. G., Durden, J. M., Drazen, J. C., Felden, J., Gates, A. R., Georgieva, M. N., Glover, A. G., Gooday, A. J., Hollingsworth, A. L., Horton, T., James, R. H., Jeffreys, R. M., & Huvenne, V. A. I. (2021). Environment, ecology, and potential effectiveness of an area protected from deep-sea mining (Clarion Clipperton Zone, abyssal pacific). *Progress in Oceanography, 197*, 102653. https://doi.org/10.1016/j.pocean.2021.102653

Kang, Y., & Liu, S. (2021). The development history and latest progress of deep-sea polymetallic nodule mining technology. *Minerals, 11*, 1132.

Kynch, G. (1952). A theory of sedimentation. *Transactions of the Faraday Society, 48*, 166–176.

Lang, A., Dasselaar, S., Aasly, K., & Larsen, E. (2019). *Technical report describing process flow overview*. Blue Nodules.

Lesage, M. (2020). *A framework for evaluating deep sea mining systems for seafloor massive sulphides deposits* (PhD thesis). Norwegian University of Science and Technology (NTNU).

MacIver, M. R. (2019). Development and usability assessment of a connected resistance exercise band application for strength-monitoring. *World Academy of Science, Engineering and Technology, 13*, 340–348. https://doi.org/10.5281/zenodo

Manning, A. J., & Dyer, K. R. (2002). A comparison of floc properties observed during neap and spring tidal. *Proceedings in Marine Science, 5*, 233–250.

Manning, A., Friend, P., Prowse, N., & Amos, C. (2007). Estuarine mud flocculation properties determined using an annular mini-flume and the LabSFLOC system. *Continental Shelf Research, 27*(8), 1080–1095.

Mehta, A. (1986). Characterisation of cohesive sediment proper- ties and transport processes in estuaries. In A. Mehta (Ed.), *Estuarine cohesive sediment dynamics* (Lecture notes in coastal and estuarine studies) (pp. 290–325). Springer.

Mewes, K., Mogollón, J. M., Picard, A., Rühlemann, C., Kuhn, T., Nöthen, K., & Kasten, S. (2014). Impact of depositional and biogeochemical processes on small scale variations in nodule abundance in the Clarion-Clipperton Fracture Zone. *Deep Sea Research Part I, 91*, 125–141. Elsevier. https://doi.org/10.1016/j.dsr.2014.06.001

Mietta, F. (2010). *Evolution of the floc size distribution of cohesive sediments* (PhD thesis). Delft University of Technology.

Mietta, F., Chassagne, C., Manning, A. J., & Winterwerp, J. C. (2009). In-fluence of shear rate, organic matter content, pH and salinity on mud flocculation. *Ocean Dynamics, 59*(5), 751–763.

Nakata, K., Kubota, M., Aoki, S., & Taguchi, K. (1997). Dispersion of resuspended sediment by ocean mining activity – Modelling study. In *Proceedings of the first international symposium on environmental studies for Deep-Sea mining, Tokyo, Japan* (pp. 169–186).

Nauru Ocean Resources Inc. (2021). *Collector test study environmental impact statement: Testing of polymetallic nodule collector system components in the NORI-D contract area, Clarion-Clipperton Zone, Pacific Ocean*, Technical report submitted to the International Seabed Authority.

Ouillon, R., Kakoutas, C., Meiburg, E., & Peacock, T. (2021). Gravity currents from moving sources. *Journal of Fluid Mechanics, 924*, A43.

Reba, I. (1966). Applications of the Coanda effect. *Scientific American, 214*(6), 84–93.

Rottman, J., & Simpson, J. (1983). Gravity currents produced by instantaneous releases of a heavy fluid in a rectangular channel. *Journal of Fluid Mechanics, 135*, 95–110.

Safar, Z., Rijnsburger, S., Sanz, M. I., Chassagne, C., Manning, A., Pietrzak, J., Souza, A., van Kessel, T., Horner-Devine, A., Flores, R., & McKeon, M. (2019). Characterization and dynamics of suspended particulate matter in the near field of the Rhine River Plume during a neap tide. In *Geophysical research abstracts* (Vol. 21).

Sanford, L. P. (1997). Turbulent mixing in experimental ecosystem studies. *Marine Ecology Progress Series, 161*, 265–293.

Shakeel, A., Safar, Z., Ibanez, M., Paassen, L., & Chassagne, C. (2020). Flocculation of clay suspensions by anionic and cationic polyelectrolytes a systematic analysis. *Minerals, 10*, 1–24.

Shakeel, A., MacIver, M. R., van Kan, P. J. M., Kirichek, A., & Chassagne, C. (2021). A rheological and microstructural study of two-step yielding in mud samples from a port area. *Colloids and Surfaces A: Physicochemical and Engineering Aspects, 624*, 126827.

Shen, X. (2016). *Modeling flocculation and deflocculation processes of cohesive sediments*. The College of William and Mary.

Smith, S. J., & Friedrichs, C. T. (2011). Size and settling velocities of cohesive flocs and suspended sediment aggregates in a trailing suction hopper dredge plume. *Continental Shelf Research, 31*(10 Suppl), S50–S63.

Spearman, J., Taylor, J., Crossouard, N., Cooper, A., Turnbull, M., Manning, A., & Lee, M. (2019). The measurement and modelling of plumes resulting from deep sea mining of Fe-Mn Crusts. In *Proceedings of the world dredging conference (WODCONXXII), Shanghai, China*.

Spearman, J., Taylor, J., Crossouard, N., Cooper, A., Turnbull, M., Manning, A., Lee, M., & Murton, B. (2020). Measurement and modelling of deep sea sediment plumes and implications for deep sea mining. *Scientific Reports, 10*(1), 1–14.

van den Bosch, G. (2023). *Tech transfer from – Supplier perspective, presented at GCE Ocean technology: Accelerating deep-sea exploration*, Bergen, Norway.

van Wijk, J. (2016). *Vertical hydraulic transport for Deep-Sea mining: A study into flow assurance* (PhD thesis). Delft University of Technology.

Volz, J. B., Mogollon, J. M., Geibert, W., Arbizu, P. M., Koschinsky, A., & Kasten, S. (2018). Natural spatial variability of depositional conditions, biogeochemical processes and element fluxes in sediments of the eastern Clarion Clipperton Zone, Pacific Ocean. *Deep Sea Research Part I: Oceanographic Research Papers, 140*, 157–172. Elsevier Ltd. https://doi.org/10.1016/j.dsr.2018.08.006

Ye, L., Manning, A. J., & Hsu, T. J. (2020). Corrigendum to Oil-mineral flocculation and settling velocity in saline water. *Water Research, 173*, 115569.

Zhao, G., Xiao, L., Yue, Z., Zhao, W., & Kou, Y. (2019). Investigation on characteristics of forces on spherical particles in Deep Sea hydraulic collecting. In *Proceedings of the 29th international Ocean and polar engineering conference*.

Zhao, G., Xiao, L., Yue, Z., Liu, M., Peng, T., & Zhao, W. (2021). Performance characteristics of nodule pick-up device based on spiral flow principle for deep-sea hydraulic collection. *Ocean Engineering, 226*, 108818.

Rudy Helmons (1987) obtained his MSc in Mechanical Engineering in 2011, after which he started as a research engineer at Royal IHC. He obtained his PhD 'cum laude' from TU Delft in 2017 on the topic of rock excavation under water conditions. After that, he started as an assistant professor in offshore and dredging engineering at TU Delft and as of February 2020, he is also an adjunct associate professor for deep sea mining at NTNU. Currently, Rudy is associate professor in Offshore and Dredging Engineering and he is active in the field of marine minerals. His research focusses on the handling of solids in a marine environment, e.g., excavation, transport, separation, and deposition. He is the project coordinator for various (deep) seabed mining research projects.

Dr. ir. Said Alhaddad is an assistant professor of offshore and dredging engineering at Delft University of Technology (TU Delft). The focus of his research is to gain a deeper understanding of the physical processes governing the interplay between underwater activities and the generation of turbidity flows.Dr. ir. Alhaddad carried out his postdoc in deep sea mining at TU Delft. He was awarded the degree of doctor from the Department of Hydraulic Engineering, Faculty of Civil Engineering and Geosciences, TU Delft. His PhD work has focused on breaching flow slides and the associated turbidity currents.

Claire Chassagne has been an associate professor at the hydraulic engineering department of the Technical University of Delft since 2020. She holds a PhD (cum laude) from the University of Leiden and a *Habilitation à Diriger des Recherces degree* from the Sorbonne University. Her research focusses on flocculation and sediment transport, the rheology of fluid mud, and the consolidation of slurries. She is a founding member of MUDNET, an academic platform for inter-disciplinary work about cohesive sediment (https://www.tudelft.nl/mudnet/), since 2015.

Mohamed Elerian (1990) has been a PhD candidate at the Dredging and Offshore Group in the Maritime Department at Delft University of Technology since 2019. He holds a Master of Science degree in Water Resources and Engineering Management from Stuttgart University. With expertise spanning both industry and academia, Mohamed's current research focuses on developing numerical-CFD models to improve the understanding of turbidity flows in general as well as the plumes and turbidity currents generated from deep-sea mining operations.

Geert Keetels is an associate professor in offshore and dredging engineering at Delft University of Technology. His research challenge is the numerical modelling of sediment transport in the range of dense soil and hyperconcentrated flows to dilute suspension on the scales that are relevant for seabed equipment. He obtained his PhD in applied physics at Eindhoven University of Technology.

Dr. Alex Kirichek is an assistant professor at the Department of Hydraulic Engineering, Faculty of Civil Engineering and Geosciences, TU Delft. His research interest is focused on developing sustainable solutions for port maintenance and sediment management strategies. He is one of the founders of MUDNET, which is an academic exchange platform for fine-grained sediment experts who are studying the physical processes (flocculation, settling, and consolidation), geophysical monitoring methods, and transport (plume propagation, density currents, and rheology) of sediment.

Laurenz Thomsen (1963) earned his PhD in 1992 from the University of Kiel, focusing on benthic boundary characteristics along continental margins. He was a postdoctoral researcher at the GEOMAR research centre in Kiel from 1992 to 1998, followed by 2 years as a Heisenberg stipend of DFG at the University of Washington in Seattle. He was a professor of geosciences at Jacobs University Bremen from 2001 to 2022 and has been professor of sedimentology at the University of Göteborg since then. He has also been an affiliate professor at the University of Washington's School of Oceanography in Seattle since 2004. His research focuses on the impact of humans on particle transport in the ocean, as well as marine robots.